



## Scholars Research Library

*J. Comput. Method. Mol. Design*, 2011, 1 (1): 26-43  
(<http://scholarsresearchlibrary.com/archive.html>)



# Computational simulation and corrosion inhibitive potential of alloxazine for mild steel in 1M HCl

N.O. Obi-Egbedi<sup>a</sup>, K.E. Essien<sup>a</sup>, I.B. Obot<sup>b,\*</sup>

<sup>a</sup>Department of Chemistry, University of Ibadan, Ibadan, Nigeria

<sup>b</sup>Department of Chemistry, Faculty of Science, University of Uyo, Uyo, Akwa Ibom State, Nigeria

## ABSTRACT

*Alloxazine (ALLO) was studied as an effective corrosion inhibitor for mild steel in 1 M HCl solution using UV-visible spectrophotometric and gravimetric technique at 303 – 333 K. The results indicate that alloxazine inhibited the corrosion process in acid medium by virtue of adsorption. Inhibition efficiency improved with concentration but decreased with rise in temperature. Temkin adsorption isotherm was found to provide an accurate description of the adsorption behaviour of the alloxazine. The mechanism of physical adsorption is proposed from the values of  $E_a$  and  $\Delta G^{\circ}_{ads}$  obtained. The UV-Visible spectroscopy study provides a strong evidence for the possibility of the formation of a complex between  $Fe^{2+}$  cation and the studied inhibitor in 1 M HCl solution which may be responsible for the observed inhibition. Computational simulation was performed on the molecular structure of alloxazine to give further insight into the inhibitory action of the inhibitor.*

**Keywords:** Adsorption isotherm, alloxazine (ALLO), mild steel, corrosion inhibition, hydrochloric acid.

## INTRODUCTION

In practice, corrosion can never be stopped but can be hindered to a reasonable level. Over the years, reductions in the rate of metal corrosion have been achieved through a number of ways. It involved controlling the pH or ion concentration of the solution or controlling the metal solution interface. This is achieved through the addition of small amount of chemicals called inhibitors, that either form a barrier like layer on the metal surface or stimulate film formation and by so doing retard or slow down the rate of metal dissolution (Khaled, 2006). Acid solutions are

widely used in industry. Some important fields of application include acid pickling of iron and steel, chemical cleaning and processing, ore production and oil well acidification. Acids such as HCl and H<sub>2</sub>SO<sub>4</sub> are generally used in the treatment of steel and ferrous alloys. Because of the general aggression of acid solutions, inhibitors are commonly used to reduce the corrosive attack on metallic materials.

Among many methods of corrosion control and prevention, the use of organic inhibitors is the most frequent used. Some researchers have shown that most of the efficient organic inhibitors contain nitrogen, oxygen, sulphur, double and triple bonds, so there is some lone pair of electrons and  $\pi$  bonds existing in their molecules which serve as adsorption sites (Obot and Obi-Egbedi, 2008). Moreover, many N-heterocyclic compounds have been used as effective inhibitors for the corrosion of metals and alloys in aqueous media (Chetouani *et al.*, 2005; Abd El-Maksoud, 2003; Wang, 2001; Popova, 2003; Obot *et al.*, 2009). Unfortunately most of the organic inhibitors are toxic, very expensive and environmentally unfriendly. Due to increasing environmental awareness and adverse effect of some chemicals, research activities in recent times are geared towards developing cheap, non-toxic and environmentally acceptable corrosion inhibitors (Obot *et al.*, 2009).

Recently, interest in alloxazines has intensified because of their important role in a wide range of biological systems (Chastain *et al.*, 1991). Lumichrome (7, 8-dimethylalloxazine), for example was found to inhibit flavin reductase in living *Escherichia coli* cells (Cunningham *et al.*, 2000). Most recently, we have reported on the corrosion inhibition action of alloxazine in sulphuric acid (Obi-Egbedi and Obot, 2011). However, there is no literature to date about the corrosion inhibitive effect of alloxazine on mild steel in HCl solution.

Thus, the inhibitory effects of alloxazine on mild steel corrosion in 1 M HCl at 303-333 K was studied by measuring weight loss with immersion time as well as by quantum chemical studies. The inhibitor adsorption mechanism was studied, and the thermodynamic functions for the dissolution and adsorption processes were calculated and discussed. The choice of this compound was also based on molecular structure considerations, i.e., this is an organic compound with several adsorption centre. The molecular structure of alloxazine is given in Figure 1.

## MATERIALS AND METHODS

### 2. Experimental Method

#### 2.1. Material

The chemical composition of mild steel samples used (Obot *et al.*, 2009) is shown in Table 1.

The mild steel sheet was mechanically press-cut into coupons of dimension 5cm x 4cm. These coupons were used as supplied without further polishing but were however ground with SiC abrasive paper, degreased in absolute ethanol, dried in acetone, weighed and stored in a moisture free desiccator prior to use (Obot and Obi-Egbedi, 2008; Obot and Obi-Egbedi, 2009).

## 2.2 Solutions

1 M HCl solution was prepared by dilution of 98% HCl (Analytical grade) using distilled water. Alloxazine was added to the acid in concentrations ranging from 0.2  $\mu\text{M}$  to 1.0  $\mu\text{M}$  and the solution in the absence of alloxazine was taken as blank for comparison. Tests were conducted under total immersion conditions in 100 ml of test solutions maintained at 303 – 333 K. The pre-cleaned and weighed coupons were immersed in beakers containing the test solutions.

To determine weight loss with respect to time, the coupons were retrieved from test solutions at 2 hrs interval progressively for 10hrs, immersed in 20% NaOH solution containing 200g $\text{l}^{-1}$  of zinc dust, scrubbed with bristle brush, washed in distilled water, dried in acetone and re-weighed (Obot *et al.*, 2009). The weight loss was taken to be the difference between the weight of the coupons at a given time and its initial weight of the test coupon determined using LP 120 digital balance with sensitivity of  $\pm 1$  mg.

## 2.3 Gravimetric measurements

The apparatus and procedure followed for the weight loss measurements were as previously reported (Abboud *et al.*, 2007; Song *et al.*, 2007; Anacona *et al.*, 2005). The corrodent concentration was kept at 1 M and the volume of the test solution used was 100 mL. All tests were made in aerated solutions. The difference between the weight at a given time and the initial weight of the coupons was taken as the weight loss which was used to compute the corrosion rate given by (Obot *et al.*, 2009)

$$\rho = \frac{\Delta W}{At} \quad (1)$$

Where,  $\Delta W$  is the Change in mass of the mild steel coupon after immersion, A is the total surface area of the mild steel coupon, t is the corrosion time and  $\rho$  is the corrosion rate.

$$\text{Surface coverage, } \theta = \frac{(\rho_1 - \rho_2)}{\rho_1} \quad (2)$$

$$\text{Inhibition efficiency, } \% I = \left( \frac{\rho_1 - \rho_2}{\rho_1} \right) \times 100 \quad (3)$$

Where  $\rho_1$  and  $\rho_2$  are the corrosion rates of the mild steel in 1 M HCl (blank) in the absence and presence of inhibitor respectively.

## RESULTS AND DISCUSSION

### 3.1 Weight loss, corrosion rate and inhibition efficiency

The weight loss (gravimetric measurements) for the mild steel in 1 M HCl containing different concentrations of the compound as function of time is presented in Fig. 2. The results show that weight loss increase with increase in time but decrease with increase in concentration of the alloxazine (ALLO). The decrease is due to the inhibitive effects of the inhibitor and these effects increase with increase in concentration of the inhibitor. The values of corrosion rate, surface coverage ( $\theta$ ) and inhibition efficiency from weight loss measurements at different concentrations

of the studied inhibitor after 10hrs immersion at 303, 313, 323 and 333 K are summarized in Table 2. It is evident from this table that the inhibition efficiency (%I) increased with increasing inhibitor concentration, reaching a maximum of 71.0%. This may be due to the adsorption of alloxazine onto the mild steel surface through non-bonding electron pairs of nitrogen and oxygen atoms as well as the  $\pi$ -electrons of the aromatic rings. The high inhibitive performance of alloxazine suggests a higher bonding ability of the inhibitor to the mild steel surface. Similar observation has been reported (Ahamad and Quraishi, 2010).

The inhibition efficiency as a function of concentration is shown in Fig. 3. The results show that as the inhibitor concentration increases, the corrosion rate decreases and therefore the inhibition efficiency increases. This implies that this inhibitor act through adsorption on mild steel surface and formation of a barrier layer between the metal and the corrosive medium. Thus, in order to confirm the adsorption of alloxazine on mild steel surface, adsorption isotherms were studied which provides basic information on the interaction of inhibitor and metal surface. Thus, the degree of surface coverage values ( $\theta$ ), at different inhibitor concentrations in 1 M HCl was evaluated from weight loss measurements at 303 K – 333 K and tested graphically for fitting to a suitable adsorption isotherm.

### 3.2 Adsorption /Thermodynamics studies

It is important to determine empirically which adsorption isotherm fits best to the surface coverage data in order to use the corrosion rate measurements to calculate the thermodynamics parameters pertaining to inhibitor adsorption. The models considered were (Tang et al., 2006; Sahin et al., 2002; Priya et al., 2008; Mu et al., 2005; Umoren et al., 2008):

$$\text{Temkin isotherm: } \exp(f\theta) = K_{ads} C \quad (4)$$

$$\text{Langmuir isotherm: } \theta = K_{ads} C \quad (5)$$

$$\text{El-Awady isotherm: } \log \frac{\theta}{1-\theta} = \log K_{ads}^{-1} + y \log C \quad (6)$$

$$\text{Freundlich isotherm: } \log \theta = \log K_{ads} + n \log C \quad (7)$$

Where  $K_{ads}$  is the equilibrium constant of the adsorption process, C the inhibitor concentration and f the factor of energetic inhomogeneity . The best fitted straight line is obtained for the plot of surface coverage ( $\theta$ ) versus logarithmic of inhibitor concentration (Log C), Fig. 4. The experimental data fit best for the Temkin adsorption isotherm as the correlation co-efficients ( $R^2$ ) were on the range  $0.9980 \geq R^2 \geq 0.9530$ . This suggests that the adsorption of alloxazine on the metal surface obeyed the Temkin adsorption isotherm. Temkin adsorption isotherm is given by;

$$\exp(-2a\theta) = K_{ads} C \quad (8)$$

Where ‘a’ is molecular interaction parameter. The calculated values of molecular interaction parameter ‘a’ and the equilibrium constant of adsorption process  $K_{ads}$  deduced from Temkin adsorption plot (Fig. 4) is also shown in Table 3. If the parameter ‘f’ is defined as:

$$f = -2a \quad (9)$$

Where  $f$  is the heterogeneous factor of the metal surface describing the molecular interactions in the adsorption layer. (Umoren *et al.*, 2008).

It is a known fact that  $K_{ads}$  denotes the strength between adsorbate and adsorbent. Large values of  $K_{ads}$  imply more efficient adsorption and hence better inhibition efficiency. It is clear from the Table 3 that values of  $K_{ads}$  are very low indicating weak interaction between the inhibitor and the mild steel surface. It seems therefore, that electrostatic interaction (Physisorption) between the inhibitor molecules existing as cations should prevail over molecular interaction which often results in strong interactions (Chemisorption) (Yurt *et al.*, 2006).

The equilibrium constant of adsorption  $K_{ads}$  is related to the standard free energy of adsorption ( $\Delta G_{ads}$ ), with the following equation (Fiala *et al.*, 2007).

$$K = \frac{1}{55.5} \exp\left(\frac{-\Delta G_{ads}}{RT}\right) \quad (10)$$

Where  $R$  is the molar gas constant,  $T$  is the absolute temperature and 55.5 is the concentration of water in solution expressed in molar.

Rearranging Equation (10) gives

$$\log K_{ads} = 1.744 - \frac{\Delta G_{ads}^{\circ}}{2.303RT} \quad (11)$$

From where the standard free energy of adsorption ( $\Delta G_{ads}^{\circ}$ ) was calculated (Table 3). The negative values of the  $\Delta G_{ads}^{\circ}$  reflect the spontaneity of the adsorption process and stability of the adsorbed layer on the mild steel surface. Generally, values of  $\Delta G_{ads}^{\circ}$  up to  $-20\text{kJ mol}^{-1}$  are consistent with electrostatic interactions between the charged molecules and the metal ( physisorption) while those around  $-40\text{kJ mol}^{-1}$  or higher are associated with chemisorptions as a result of sharing or transfer of electrons from organic molecules to the metal surface to form a coordinate type of bond (chemisorptions) (Umoren *et al.*, 2008). One can see that the calculated  $\Delta G_{ads}^{\circ}$  values are less than  $-20\text{kJ mol}^{-1}$ , indicating, therefore that the adsorption mechanism of the alloxazine on mild steel in 1 M HCl solution was typical of physisorption (Table 3).

### 3.3 Temperature Effect

The effect of temperature on the corrosion rate of mild steel in 1 M HCl solution in absence and presence of 0.2  $\mu\text{M}$  to 1.0  $\mu\text{M}$  of alloxazine was studied at different temperatures (303-333 K) by weight loss measurements. This effect of temperature on the inhibited acid-metal reaction is very complex, because many changes occur on the metal surface such as rapid etching, desorption of inhibitor and the inhibitor itself may undergo decomposition (Bentiss *et al.*, 2005). The data of Table 2 shows that the %*I* decrease as the temperature increases and with decrease in concentrations of studied inhibitor. Fig. 3 shows the variation of percentage inhibition efficiency with temperature. It is clear from the figure that percentage inhibition efficiency increases with alloxazine concentration but decreases with increase in temperature. This may be probably due to

increased rate of desorption of alloxazine from the mild steel surface at higher temperature (Li et al., 2010; Obot and Obi-Egbedi, 2010a).

In acidic solution, the corrosion rate is related to temperature by Arrhenius equation (Behpour et al., 2009).

$$\log \rho = \log A - \frac{E_a}{2.303RT} \quad (12)$$

Where  $\rho$  is the corrosion rate determined from the weight loss measurement,  $E_a$ , the apparent activation energy,  $A$  the Arrhenius constant,  $R$  the molar gas constant and  $T$  is the absolute temperature. The apparent activation energy,  $E_a$  was determined from the slopes of  $\log \rho$  versus  $1/T$  graph depicted in Fig. 5.

The values of activation energies were calculated and given in Table 4. These values indicate that the presence of alloxazine increases the activation energy of the metal dissolution reaction. The increase in  $E_a$  is proportional to the inhibitor concentration. The increase in activation energy can be attributed to an appreciable decrease in the adsorption of the inhibitor on the mild steel surface with increase in temperature and a corresponding increase in corrosion rates due to the fact that greater area of metal is exposed to the acid environment (Szauer and Brand, 1981). The adsorption of the studied inhibitor is assumed to occur on the higher energy sites and the presence of the inhibitor, which results in the blocking of the active sites, must be associated with an increase in the activation energy of mild steel corrosion in the inhibited state (Fouda et al., 2006). The higher value of  $E_a$  in the presence of inhibitor compared to that in its absence and the decrease in the  $\%I$  with rise in temperature is interpreted as an indication of physisorption (Umoren and Ebenso, 2007). The values of enthalpy of activation  $\Delta H^*$  and entropy of activation  $\Delta S^*$  were obtained from the transition state equation (Abboud et al., 2007).

$$\rho = \left( \frac{RT}{Nh} \right) \exp\left( \frac{\Delta S^*}{R} \right) \exp\left( \frac{-\Delta H^*}{RT} \right) \quad (13)$$

Where  $\rho$  is the corrosion rate,  $h$  is the plank's constant ( $6.6261 \times 10^{-34}$  Js);  $N$  is the Avogadro's number ( $6.02252 \times 10^{23} \text{ mol}^{-1}$ );  $T$  is the absolute temperature and  $R$  is the universal gas constant. A plot of  $\log(\rho/T)$  as a function of  $1/T$  (Fig. 6) was made for mild steel corrosion in 1 M HCl in the absence and presence of different concentrations of alloxazine. Straight lines were obtained with slope of  $(\Delta H^*/2.303R)$  and an intercept of  $[\log(R/Nh) + (\Delta S^*/2.303R)]$  from which the values of  $\Delta H^*$  and  $\Delta S^*$ , respectively, were computed and listed also in Table 4. Examination of these data reveals that the  $\Delta H^*$  values for dissolution reaction of mild steel in 1 M HCl in the presence of alloxazine are higher ( $1.55 - 2.49 \text{ kJ mol}^{-1}$ ) than that in the absence of ALLO ( $0.92 \text{ kJ mol}^{-1}$ ). The positive sign of  $\Delta H^*$  show the endothermic nature of the solution process suggesting that the dissolution of mild steel is slow which indicates that inhibition efficiencies decrease with increase in temperature (Guan et al., 2004; Abboud et al., 2007). It is also clear from Table 4 that  $E_a$  and  $\Delta H^*$  increase with increase in alloxazine concentration.



The entropy of inhibitor adsorption ( $\Delta S_{\text{ads}}^*$ ) was negative because inhibitor molecules, freely moving in the bulk solution were adsorbed in an orderly fashion onto the mild steel surface, resulting in a decrease in entropy (Mu *et al.*, 2005). This implies that, the activated complex in the rate determining step represents association rather than dissociation step, meaning that a decrease in disordering takes place on going from reactants to the activated complex (Herrag *et al.*, 2010).

### 3.4 UV-Visible spectroscopic investigation

The absorption of monochromatic light is a suitable method for identification of complex ions, the absorption of light is proportional to the concentration of the absorbing species (Abboud *et al.*, 2007). Since there is often a certain quantity of metal cation in the solution that is first dissolved from the metal surface, such procedures were conducted in the present work to confirm the possibility of the formation of [ALLO-Fe<sup>2+</sup>] complexes as described in several publications (Sherif and Park, 2005; Rangelov and Mircheva, 1996; Elmorsi and Hassanein, 1999; Abdel-Gaber *et al.*, 2009). Furthermore, the change in position of the absorbance maximum and change in the value of absorbance indicate the formation of a complex between two species in solution (Abboud *et al.*, 2007). For routine analysis a simple conventional technique based on UV-visible absorption spectra obtained from 1 M HCl solution containing 1.0  $\mu$  M alloxazine before and after 3 days of mild steel immersion is shown in Fig. 7.

The absorption spectrum of the solution containing 1.0  $\mu$ M alloxazine before the mild steel immersion shows a band of shorter wavelength while that of 3 days of steel immersion shows a band of longer wavelength (Fig. 7). The electronic absorption spectra of ALLO before the steel immersion display a main visible band at 330 nm. This band may be assigned to  $\pi$ - $\pi^*$  transition involving the whole electronic structure system of the compound with a considerable charge transfer character (Abboud *et al.*, 2009). After three days of steel immersion (Fig. 7), it is clearly seen that the band maximum underwent a blue shift, suggesting the interaction between ALLO and Fe<sup>2+</sup> ions in the solution (Abboud *et al.*, 2007). Furthermore, there is a slight increase in the absorbance of this band. It is clear that there was no significant difference in the shape of the spectra before and after the immersion of ALLO showing a possibility of weak interaction between ALLO and mild steel (Physisorption) (Obi-Egbedi and Obot, 2010). This indicates that the nitrogen and the carbonyl groups are weakly held up in the complex with iron (Song *et al.*, 2007). These experimental findings provide a strong evidence for the possibility of the formation of a complex between Fe<sup>2+</sup> cation and the studied inhibitor in 1 M HCl solution (Anacona, 2005).

### 3.5 Quantum Chemical Calculations

Quantum chemical calculations have proved to be a very powerful tool for studying corrosion inhibition mechanism (Anacona, 2005). Thus, a theoretical study was undertaken to observe its possible physical characters which could contribute to inhibition. Recently, the density functional theory (DFT) has been used to analyze the characteristics of the inhibitor/surface mechanism and to describe the structural nature of the inhibitor on the corrosion process (Lashkari and Arshadim, 2004; Sein *et al.*, 2001; Ebenso *et al.*, 2010). Thus in the present investigation, quantum chemical calculation using DFT was employed to explain the experimental results obtained in this study and to further give insight into the inhibition action of ALLO on the mild steel surface.

The calculated values of the quantum chemical parameters obtained using the Hartree-fock/Density functional theory (HF-DFT) by Becke 3 Lee Yang Parr (B3LYP) method with 6-31G\* basis set of SPARTAN' 06 V112 program are presented in Table 5. The relation between inhibition efficiency of inhibitor and the quantum chemical calculation parameters like  $E_{\text{HOMO}}$ ,  $E_{\text{LUMO}}$ , dipole moment and  $\Delta E$  were investigated. These parameters provide information about the reactive behavior of molecules. These theoretical parameters were calculated in the neutral as well as in the protonated form of ALLO in the aqueous phase. The reactive ability of the inhibitor is considered to be closely related to their frontier molecular orbitals, the HOMO and LUMO (Obi-Egbedi and Obot, 2010). The highest occupied molecular orbital (HOMO) is usually the region of high electron density, therefore is often associated with the electron donating ability of the molecule. The optimized geometry of alloxazine is shown in Fig. 8.

As we know, frontier orbital theory is useful in predicting the adsorption centers of the inhibitors responsible for the interaction with surface metal atoms. The HOMO and the LUMO population of alloxazine were plotted and are shown in Figs. 9-10 respectively. It could also be easily seen that the frontier orbitals, the HOMO and the LUMO were distributed around the entire molecule.

Moreover, the gap between the LUMO and HOMO energy levels of the molecule was another important factor that should be considered. It has been reported that excellent corrosion inhibitors are usually those organic compounds that are not only offer electrons to unoccupied orbital of the metal but also accept free electrons from the metal (Chao et al., 2005). It is also well documented in literature that the higher the HOMO energy of the inhibitor, the greater its ability of offering electrons to unoccupied d-orbital of the metal, and the higher the corrosion inhibition efficiency. It is evident from Table 5 that ALLO has the highest  $E_{\text{HOMO}}$  in the neutral form and a lower  $E_{\text{HOMO}}$  in the protonated form. This means that the electron donating ability of ALLO is weaker in the protonated form. This confirms the experimental results that interaction between ALLO and mild steel is electrostatic in nature (physisorption). In addition, the lower the LUMO energy, the easier the acceptance of electrons from metal surface, as the LUMO-HOMO energy gap decreased and the efficiency of inhibitor improved. It is clear from Table 5 that the protonated form of ALLO exhibits the lowest  $E_{\text{LUMO}}$ , making the protonated form the most likely form for the interaction of mild steel with ALLO molecule. Low values of the energy gap ( $\Delta E$ ) will provide good inhibition efficiencies, because the excitation energy to remove an electron from the last occupied orbital will be low (Gece, 2008). A molecule with a low energy gap is more polarizable and is generally associated with a high chemical reactivity, low kinetic stability and is termed soft molecule (Dwivedi and Misra, 2010). The adsorption of inhibitor onto a metallic surface occurs at the part of the molecule which has the greatest softness and lowest hardness (Wang et al., 2007). Quantum chemical parameters listed in Table 5 indicate that alloxazine is a good inhibitor in HCl which corresponds to the experimental results.

The Mulliken charge distribution of alloxazine is presented in Fig. 11. It has been reported that the more negative the atomic charges of the adsorbed centre, the more easily the atom donates its electron to the unoccupied orbital of the metal (Xia et al., 2008). It is clear from Fig. 11 that Nitrogen and Oxygen as well as some carbons atoms carries negative charge centers which could offer electrons to the mild steel surface to form a coordinate bond. It could be readily observed



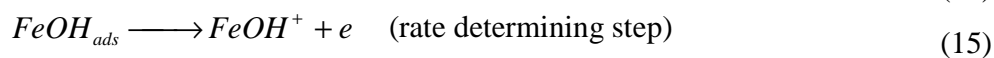
that oxygen and the nitrogen atoms had higher charge densities and might form the adsorption centers.

In acidic solution, this studied inhibitor can exist as cationic species through the protonation of nitrogen and oxygen atoms. The protonated compound (Fig. 12) can be adsorbed on the metal surface by means of electrostatic interaction between  $Cl^-$  (which act as a bridge between the metal surface and the electrolyte) and protonated alloxazine. Moreover, the adsorption of these compound on the anodic sites through lone pair of electrons on N and O atoms and through the  $\pi$ -electrons of the phenyl groups will then reduces the anodic dissolution of mild steel (Obot *et al.*, 2009). The dipole moment is another important electronic parameter that results from non-uniform distribution of charges on the various atoms in a molecule. It is mainly used to study the intermolecular interactions involving the Van der Waals type dipole-dipole forces etc, because the larger the dipole moment the stronger will be the intermolecular attraction (Dwivedi and Misra, 2010). The dipole moment of ALLO (Table 5) is highest in the protonated form. The high value of dipole moment probably increases the adsorption between chemical compound and metal surface (Li *et al.*, 2009). The values of dipole moment indicate the possibility of adsorption of studied compound by electron donation to the unfilled orbital of iron. The electronic configuration of iron is  $[Ar] 4s^2 3d^6$ , so 3d orbital is not fully filled with electrons. Accordingly, the adsorption of ALLO molecules can be regarded as a quasi-substitution process between the ALLO compound and water molecules at the mild steel surface (Obi-Egbedi and Obot, 2010b).

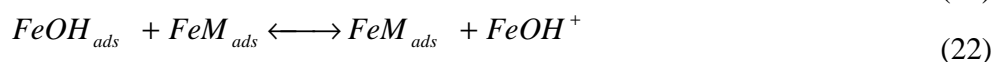
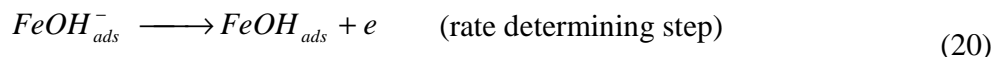
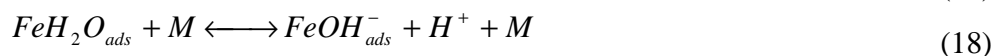
From the above discussion, it could be deduced that alloxazine interact with the mild steel surface using a number of active centers forming a good protective layer on the mild steel surface, thus retarding further corrosion of the metal in hydrochloric acid solution. It also exists in the cationic form which can interact with mild steel surface by electrostatic attraction.

### 3.6 Mechanism of Corrosion Inhibition

A number of mechanistic studies on the anodic dissolution of Fe in acidic solutions have been undertaken, and the hydroxyl accelerated mechanism proposed initially by Bockris and Drazie (1962) and reported by Oguzie (2004) has gained overwhelming acceptance:



It has been suggested that anions such as  $Cl^-$ ,  $I^-$ ,  $SO_4^{2-}$  and  $S^{2-}$  may also participate in forming reaction intermediates on the corroding metal surface, which either inhibit or stimulate corrosion (Hurlen *et al.*, 1984). It is important to recognize that the suppression or stimulation of the dissolution process is initiated by the specific adsorption of the anions on the metal surface. According to the Bockris mechanism outlined earlier, Fe electro-dissolution in acidic sulphate solutions depends primarily on the adsorbed intermediate  $FeOH_{ads}$ . Ashassi-Sorkhabi and Nabavi-Amri (2000) proposed the following mechanism involving two adsorbed intermediates to account for the retardation of Fe anodic dissolution in the presence of an inhibitor:



Where M represents the inhibitor species

Considering the inhomogeneous nature of metallic surfaces resulting from the existence of lattice defects and dislocations, a corroding metal surface is generally characterized by multiple adsorption sites having activation energies and heats of adsorption. Inhibitor molecules may thus be adsorbed more readily at surface sites having suitable adsorption enthalpies. According to the detailed mechanism above, displacement of some adsorbed water molecules on the metal surface by inhibitor species to yield the adsorbed intermediate  $FeM_{ads}$  (Eq. 19) reduces the amount of the species  $FeOH_{ads}^-$  available for the rate determining steps and consequently retards Fe anodic dissolution (Obot and Obi-Egbedi, 2010a; Omar and Mokhtar, 2010).

From the experimental and theoretical results obtained, we note that a plausible mechanism of corrosion inhibition of mild steel in 1.0 M HCl by alloxazine may be deduced on the basis of adsorption. The adsorption process is affected by the chemical structures of the inhibitor, the nature and charged surface of the metal and the distribution of charge over the whole inhibitor molecule. In general, owing to the complex nature of adsorption and inhibition of a given inhibitor, it is impossible for single adsorption mode between inhibitor and metal surface.

Thus, in aqueous acidic solutions, the ALLO exists either as neutral molecules or in the form of protonated ALLO (cations). ALLO may adsorb on the metal/acid solution interface by one and/or more of the following ways: (i) electrostatic interaction of protonated ALLO with already adsorbed chloride ions, (ii) donor-acceptor interactions between the  $\pi$ -electrons of aromatic ring and vacant d orbital of iron surface atoms, (iii) interaction between unshared electron pairs of O and N atoms of ALLO and vacant d orbital of iron surface atoms (Obi-Egbedi and Obot, 2010).

Generally, two modes of adsorption could be considered. In one mode, the neutral ALLO molecules may be on the surface of mild steel through the chemisorption mechanism involving the displacement of water molecules from the mild steel surface and the sharing of electrons between the heteroatoms and iron. The inhibitor molecule can also adsorb on the mild steel surface on the basis of donor-acceptor interactions between  $\pi$ -electrons of the heterocyclic ring and vacant d-orbitals of surface iron. In another mode, since it is well known that the steel surface bears positive charge in acid solution (Mu et al., 1996), it is difficult for the protonated

ALLO to approach the positively charged mild steel surface ( $H_3O$  / metal interface) due to the electrostatic repulsion.

**Table 1: Chemical Composition of Mild Steel Samples (Wt %).**

|    |        |
|----|--------|
| C  | 0.17   |
| Si | 0.26   |
| Mn | 0.46   |
| P  | 0.0047 |
| S  | 0.017  |
| Fe | Bal.   |

**Table 2. Corrosion parameters for mild steel in 1 M HCl in the absence and presence of different concentrations of alloxazine at different temperatures**

| Concentration of Alloxazine ( $\mu\text{M}$ ) | Corrosion rate, inhibition efficiency (% I) and degree of surface coverage ( $\theta$ ) |    |      |                    |    |      |                    |    |      |                    |    |      |
|---|---|----|------|--------------------|----|------|--------------------|----|------|--------------------|----|------|
|   | 303 K   |    |      | 313 K              |    |      | 323 K              |    |      | 333 K              |    |      |
|   | $a \times 10^{-4}$  | b  | c    | $a \times 10^{-4}$ | b  | c    | $a \times 10^{-4}$ | b  | c    | $a \times 10^{-4}$ | b  | c    |
| Blank   | 9.89  | -  | -    | 10.1               | -  | -    | 11.3               | -  | -    | 15.1               | -  | -    |
| 0.2   | 6.37  | 36 | 0.36 | 7.52               | 24 | 0.24 | 8.29               | 23 | 0.23 | 12.8               | 15 | 0.15 |
| 0.4   | 5.93  | 40 | 0.40 | 6.43               | 35 | 0.35 | 8.16               | 28 | 0.28 | 11.6               | 23 | 0.23 |
| 0.6   | 4.28  | 57 | 0.57 | 4.95               | 50 | 0.50 | 7.24               | 36 | 0.36 | 10.3               | 32 | 0.32 |
| 0.8   | 3.31  | 67 | 0.67 | 4.06               | 59 | 0.59 | 6.00               | 47 | 0.47 | 8.84               | 42 | 0.42 |
| 1.0   | 2.84  | 71 | 0.71 | 3.24               | 67 | 0.67 | 4.29               | 55 | 0.55 | 7.44               | 51 | 0.51 |

(a) Corrosion rate obtained from equation (1); (b) Inhibition efficiency (%I) obtained using equation (2); (c) Degree of surface coverage ( $\theta$ ) obtained using equation (3).

**Table 3: Adsorption parameters from Temkin isotherm for Mild steel coupons in 1M HCl containing different concentration at 303-333 K.**

| Inhibitor | Temperature (K) | Adsorption parameters |       |       |               |        |
|-----------|-----------------|-----------------------|-------|-------|---------------|--------|
|           |                 | $K_{ads}$ (mol/L)     | $f$   | $A$   | $-AG(KJ/mol)$ | $R^2$  |
| DAQ       | 303             | 5.12                  | 10.31 | -5.16 | 16.637        | 0.9530 |
|           | 313             | 3.57                  | 9.09  | -4.55 | 13.763        | 0.9860 |
|           | 323             | 4.73                  | 12.05 | -6.03 | 14.959        | 0.9850 |
|           | 333             | 1.79                  | 10.99 | -5.50 | 12.732        | 0.9980 |

Thus, the presence of chloride ions which have excess negative charges in the vicinity of the interface could favour the adsorption of the positively charged inhibitor molecules. The protonated ALLO could then adsorb through electrostatic interactions between the positively charged molecules and the steel surface which now has negatively charged chloride ions on it.

Thus, there is a synergism between  $\text{Cl}^-$  ions and the protonated ALLO molecules. Similar mechanism has been proposed recently (Ahmad *et al.*, 2010; Obi-Egbedi and Obot, 2010).

**Table 4: Activation parameters for Mild steel coupons in 1 M HCl containing different concentration of alloxazine at 303-333 K**

| Concentration     | Ea (kJ mol <sup>-1</sup> ) | $\Delta H^*$ (kJ/mol) | $-\Delta S^*(\text{J/molK}^{-1})$ |
|-------------------|----------------------------|-----------------------|-----------------------------------|
| Blank             | 1.11                       | 0.92                  | 299.6                             |
| 0.2 $\mu\text{M}$ | 1.86                       | 1.55                  | 300.6                             |
| 0.4 $\mu\text{M}$ | 1.86                       | 1.61                  | 301.1                             |
| 0.6 $\mu\text{M}$ | 2.45                       | 2.18                  | 301.3                             |
| 0.8 $\mu\text{M}$ | 2.80                       | 2.49                  | 302.4                             |
| 1.0 $\mu\text{M}$ | 2.84                       | 2.49                  | 304.4                             |

**Table 5: Quantum parameters obtained by Spartan'06**

| Quantum parameter                        | Neutral calculated value |  | Protonated calculated value |  |
|--|--------------------------|--|-----------------------------|--|
|  | ALLO                     |  | ALLO                        |  |
| $E_{\text{HOMO}}$ (eV)                   | -6.781                   |  | -10.764                     |  |
| $E_{\text{LUMO}}$ (eV)                   | -2.736                   |  | -6.799                      |  |
| $E_{\text{LUMO}} - E_{\text{HOMO}}$ (eV) | 4.044                    |  | 3.964                       |  |
| Heat of Formation (kJ/mol)               | -754.205                 |  | -754.586                    |  |
| CPK area ( $\text{\AA}^2$ )              | 207.530                  |  | 211.735                     |  |
| CPK volume ( $\text{\AA}^3$ )            | 191.397                  |  | 195.012                     |  |
| Dipole moment (Debye)                    | 4.262                    |  | 7.98                        |  |
| Molecular weight (amu)                   | 214.184                  |  | 214.191                     |  |

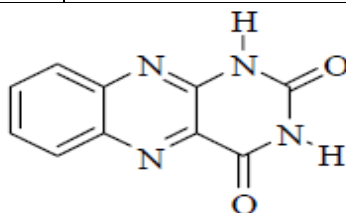


**Fig. 1. Molecular structure of alloxazine (ALLO).**

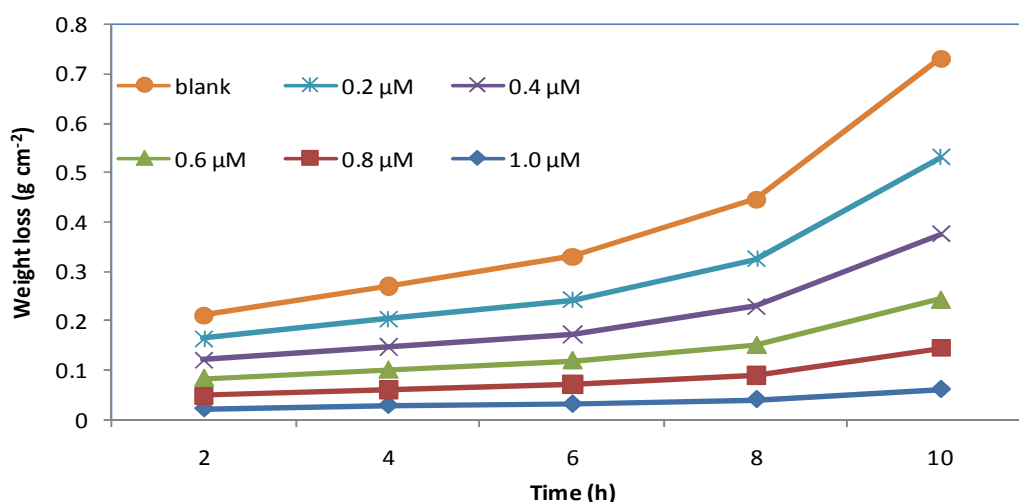


**Figure 2. Plot of weight loss ( $\text{g cm}^{-2}$ ) versus time (h) in the absence and presence of different concentrations of alloxazine at 303 K.**

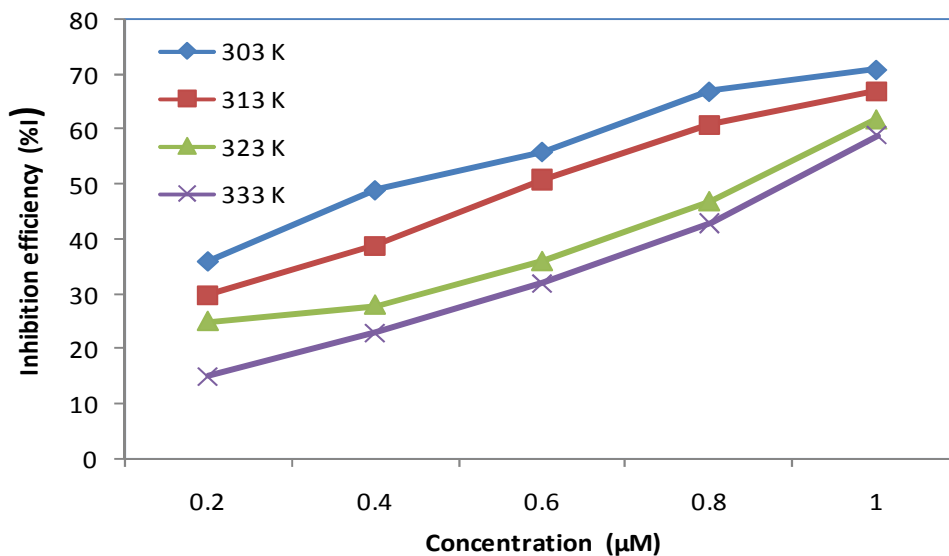


Figure 3. Plot of Inhibition efficiency (%I) versus concentrations of alloxazine at different temperatures.

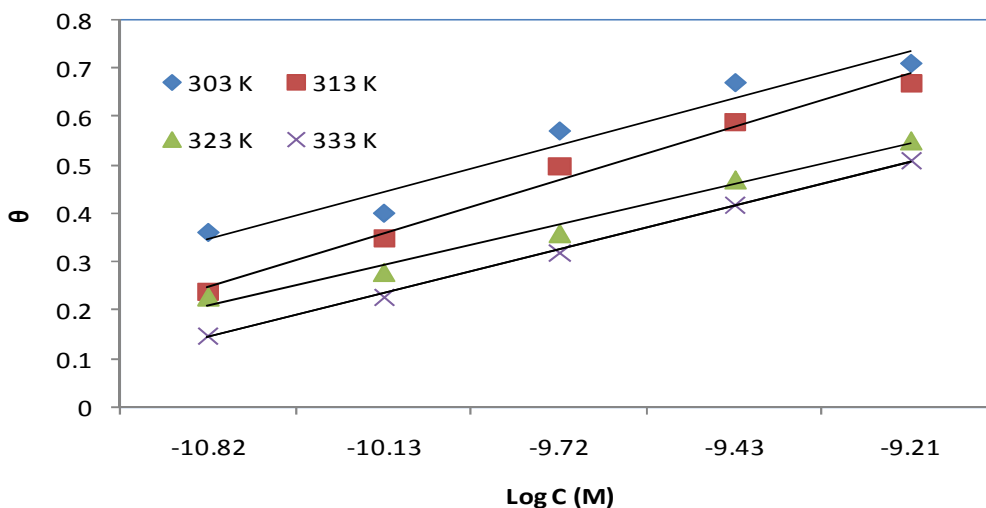
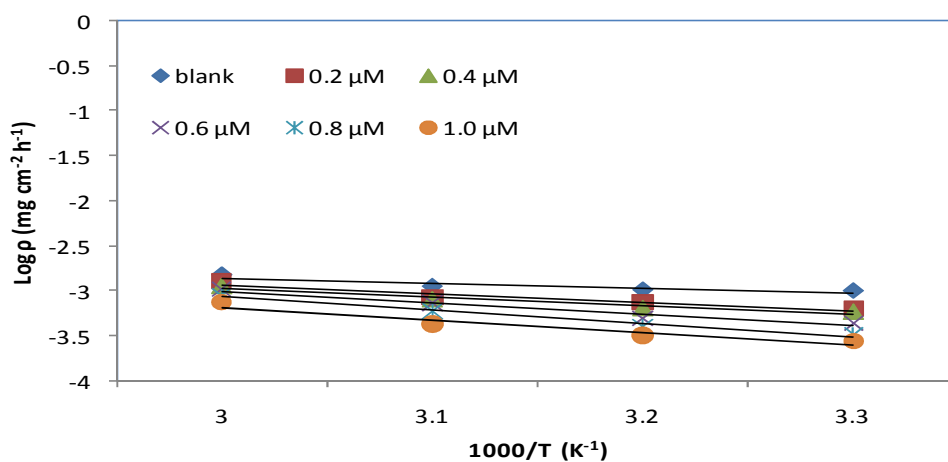
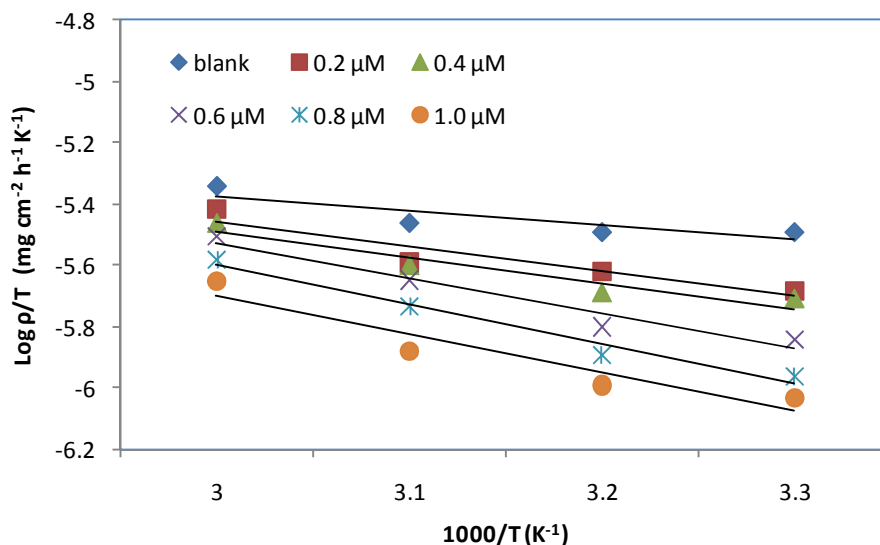


Figure 4. Temkin adsorption isotherm plot as  $\theta$  versus Log C for alloxazine at 303-333 K.



**Figure 5: Arrhenius plot as log  $\rho$  versus  $1/T$  for mild steel coupons in 1 M HCl containing different concentration of alloxazine.**



**Figure 6: Transition State plot as log (CR/T) versus  $1/T$  for mild steel coupons in 1 M HCl containing different concentration of alloxazine.**

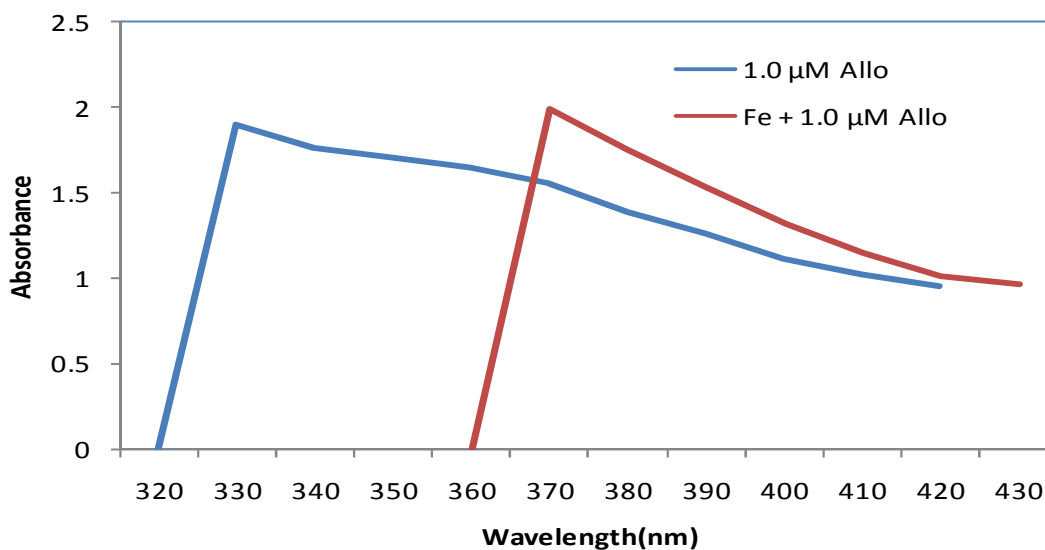


**Figure 7. Uv-visible spectra of the solution containing 1M HCl in 1.0 μM alloxazine before (blue) and after (red) mild steel immersion.**



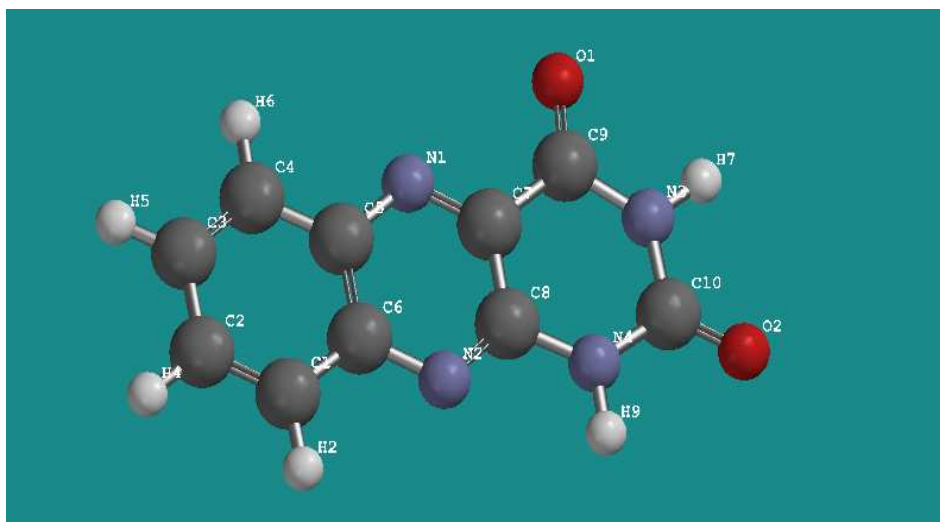


**Figure 8. DFT-B3LYP Optimized Structure of alloxazine**

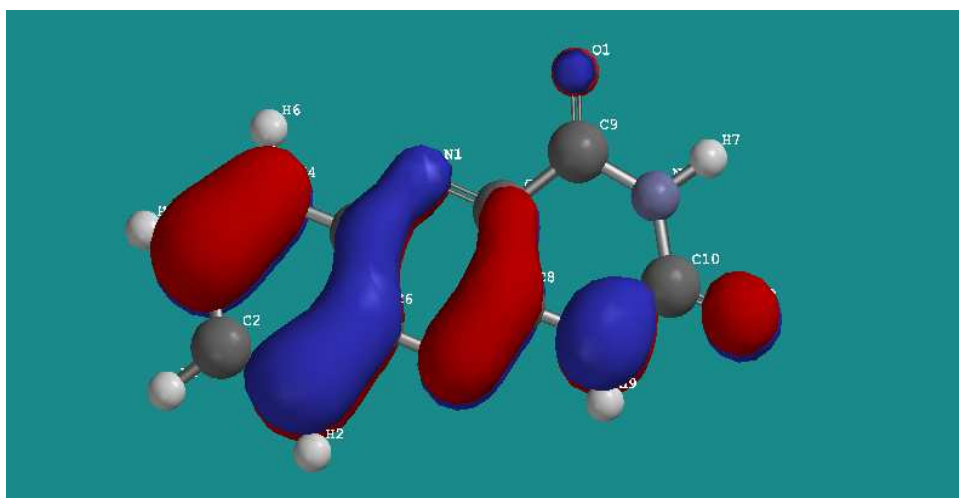


**Figure 9. HOMO electronic density of alloxazine molecule**

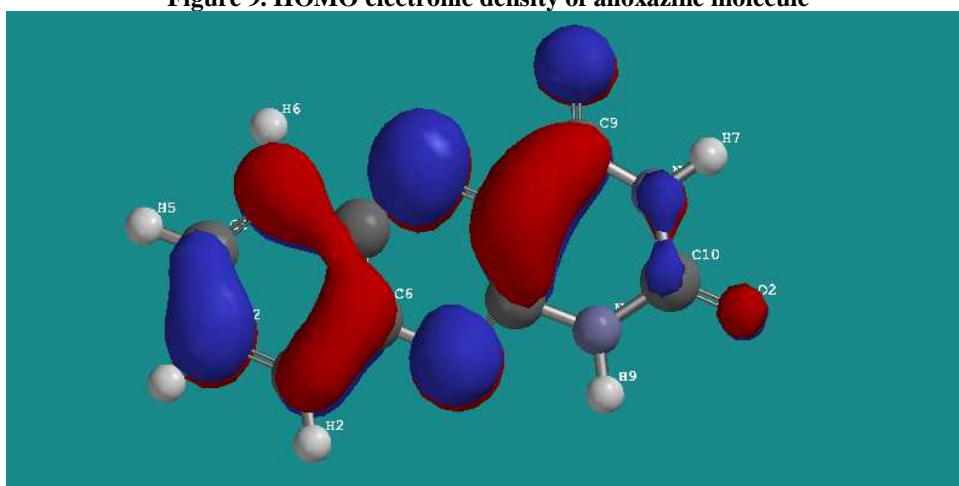


**Figure 10. LUMO electronic density of alloxazine molecule**

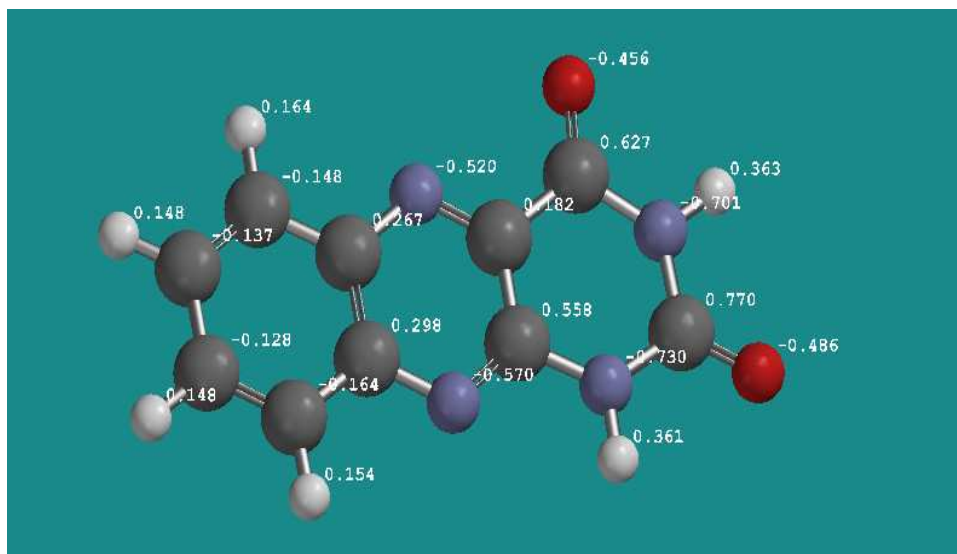


**Figure 11. Mulliken Charges of the atoms in alloxazine**

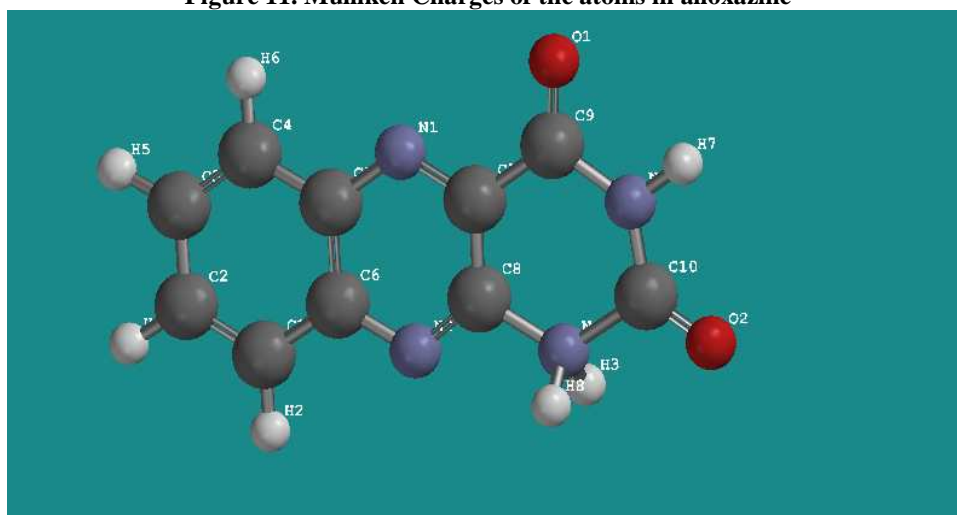


**Figure 12. Optimized structure of alloxazine protonated at N2**

## CONCLUSIONS

1. Results obtained from the experimental and theoretical data show that alloxazine acts as an effective inhibitor of mild steel corrosion in 1 M HCl.
2. The corrosion process was inhibited by adsorption of the organic matter on the steel surface.
3. Inhibition efficiency Increases with increase in the concentration of the alloxazine but decreases with rise in temperature.
4. The adsorption of alloxazine on mild steel surface from 1 M HCl obeys the Temkin adsorption isotherm.

5. Phenomenon of physical adsorption is proposed from the values of kinetic/thermodynamics parameters ( $E_a$ ,  $\Delta G_{ads}^{\circ}$ ) obtained.
6. The UV-Vis studies clearly reveal the formation of complex which may be also responsible for the observed inhibition.
7. Quantum chemical calculations show that apart from studied compound molecule adsorbing as cationic species on the mild steel surface, it can also adsorbed as molecular species using oxygen, nitrogen and benzylic carbons as its active centers.

## REFERENCES

- [1] Abboud, Y., Abourriche, A., Saffaj, T., Berrada, M., Charrouf, M., Bennamara, A., Al-Himidi, N., Hannache, I., **2007**. *Mater. Chem. Phys.* 105, 1.
- [2] Abboud, Y., Abourriche, A., Ainane, T., Charrouf, M., Bennamara, A., Tanane, O., Hammouti, B., **2009**. *Chem. Eng. Comm.* 196, 788.
- [3] Abdel-Gaber, A. M., Abd-ElNabey, B. A., Sidahmed, I. M., El-Zayady, A. M., Saadawy, M., Abboud, Y., Abourriche, A., Saffaj, T., Berrada, M., Charrouf, M., Bennamara, A., Hannache, H., **2009**. *Desalination*. 237, 175.
- [4] Abd El-Maksoud, S. A., **2003**. *Appl. Surf. Sci.* 206,129.
- [5] Ahamad, I., Prasad, R., Quraishi, M. A., **2010**. *Corros. Sci.* 52, 1472.
- [6] Ahamad, I. and Quraishi, M. A., **2010**. *Corros. Sci.* 52, 651.
- [7] Anacona, J. R., Martell, T., Sanchez, I.,**2005**. *J.chin. Chem. Soc.* 50, 375.
- [8] Ashassi-Sorkhabi, H., Nabavi-Amri, S. A., **2000**. *Acta Chim. Slov.* 47, 512.
- [9] Behpour, M., Ghoreishi, S. M., Gundomi-Niasar, A., Soltani, N., Salavati-Niasari. M. J., **2009**. *Mater. Sci.* 44, 2444.
- [10] Bentiss, F., Lebrini, M., Lagrenee, M., **2005**. *Corros. Sci.* 47, 2915.
- [11] Bockris, J. O. M., Drazie, D., **1962**. *Electrochim. Acta* 7, 293.
- [12] Chetouani, A., Hammouti, Benhadda, B. T., Daoudi, M., **2005**. *Appl. Surf. Sci.* 249, 375.
- [13] Choa, P., Liang, Q., Li, Y., **2005**. *Appl. Surf. Sci.* 252, 1596.
- [14] Cunningham, O., Gore, M.G., Mantle, T. J., **2000**. *Biochem. J.* 345, 393.
- [15] Chastain, J., McCormick, D.B., Flavin Metabolites, in *Chemistry and Biochemistry of Flavoenzymes*, 1, ed. F. Muller, CRC Press, Boston, **1991**, pp. 196.
- [16] Dwivedi, A., Misra, N., **2010**. *Der pharma. Chem.* 2, 58.
- [17] Ebenso, E. E., Arslan, T., Kandemirli, F., Caner, N., Love, I., **2010**. *Int. J. Quant. Chem.* 110, 1003.
- [18] Elmorsi, M. A., Hassanein. M. A., **1999**. *Corros. Sci.* 41, 2337.
- [19] Fiala, A., Chibani, A., Darchen, A., Boulkamh, A., Djebbar, K., **2007**. *Appl. Surf. Sci.* 253, 9347.
- [20] Founda, A. S., Abd El-Aal, A., Kandil, A. B. **2006**. *Desalination*. 201: 216.
- [21] Gece, G., **2008**. *Corros. Sci.* 50, 2981.
- [22] Guan, N. M., Xueming, I., Fei, I., **2004**. *Mater. Chem. Phys.* 86, 59.
- [23] Herrag, L., Hammouti, B., Elkadri, S., Aouniti, A., Jama, C., Vezin, H., Bentiss, F., **2010**. *Corros. Sci.* doi:10.1016/j.Corsci.2010.05.024.
- [24] Hurlen, T., Lian, H., Odegard, O. S., Valand, T., 1984. *Electrochim. Acta* 29, 579.
- [25] Jacobson, G. A. **2009**. *The AMPTLAC Quarterly*, 1(4), 39.
- [26] Khaled, K. F., **2006**. *Appl. Surf. Sci.* 252, 4120.

- [27] Lashkari, M., Arshadi, M. R. J., **2004**. *Chem. Phys.* 299, 131.
- [28] Li, X., Deng, S., Fu, H., **2010**. *Prog. Org. Coat.* 67, 420.
- [29] Mu, G. N., Zhao, T. P., Liu, M., Gu, T., **1996**. *Corrosion* 52, 853.
- [30] Mu, G. N., Li, X. M., Liu, G. H., **2005**. *Corros. Sci.* 47, 1932.
- [31] Obi-Egbedi, N. O., Obot, I. B., **2010**. *Arabian Jour. Chem.* doi:10.1016/J.arabjc.2010.10.004.
- [32] Obi-Egbedi, N. O., Obot, I.B. **2011**. *Corros. Sci.* 53, 263.
- [33] Obot, I. B., Obi-Egbedi, N. O., **2010a**. *Curr. Appl. Phys.* doi:10.1016/j.cap.2010.08.007.
- [34] Obot, I.B., Obi-Egbedi, N. O., **2010b**. *Corros. Sci.* 52, 198.
- [35] Obot, I.B., Obi-Egbedi, N. O., Odozi, N. W., **2009**. *Corros. Sci.* doi: 10. 1016/j Corsci. 2009. 11.013.
- [36] Obot, I. B., Obi-Egbedi, N. O., **2009**. *Corros. Sci.* doi: 10. 1016/j Corsci:2009.10.017.
- [37] Obot, I. B., Obi-Egbedi, N. O., **2008**. *Colloid Surf A: physicochem. Eng. Aspects* 330, 207.
- [38] Oguzie, E. E., **2004**. *Mater. Chem. Phys.* 87, 212.
- [39] Omar, B., Mokhtar, O., **2010**. *Arab. J. Chem.*, doi:10.1016/j.arabjc.2010.07.016.
- [40] Popova, A., Christov, M., *Dellgeorigiev, T.*, **2003**. *Corros. Sci.* 59, 756.
- [41] Priya, A. R., Muralidharam, V. S., Subramania, A., **2008**. *Corrosion* 64, 541.
- [42] Rangelov, S., Mircheva, V., **1996**. *Corros. Sci.* 38, 301.
- [43] Sahin, M., Bilgic, S., Yilmaz H., **2002**. *Appl. Surf. Sci.* 195, 1.
- [44] Sein, T. L., Wei, Y., Jansen, S. A., **2001**. *Comput. Theor. Polym. Sci.* 11, 83.
- [45] Sherif, E. M., Park, S. M. J., **2005**. *Electrochem. Soc.* 152, B428.
- [46] Song, X. Q., Wang, Y. W., Zheng, J. R., Liu, W. S., Tan, M. Y., **2007**. *Spectrochim. Acta*, part A. in press.
- [47] Szauer, T., Brand. A., **1981**. *Electrochim. Acta* 26, 245.
- [48] Tang, L., Li, X., Si, Y., Mu, G., Liu, G.H., **2006**. *Mater. Chem. Phys.* 95, 26.
- [49] Umoren, S.A., Obot, I.B., Ebenso, E.E., Okafor, P.C., **2008**. *Port. Electrochim. Acta* 26, 267.
- [50] Umoren, S. A., Ebenso, E. E., **2007**. *Mater. Chem. Phys.* 106, 393.
- [51] Wang, I., **2001**. *Corros. Sci.* 43, 2281.
- [52] Wang, H., Wang, X., Wang, H., Wang, L., Liu. A., **2007**. *J. Mol. Model* 13, 147.
- [53] Xia, S., Qiu, M., Yu, L., Liu, F., Zhao, H., **2008**. *Corros. Sci.* 50, 2021.
- [54] Yurt, A., Ulutas, S., Dal, H. *Appl. Surf. Sci.* 253 (2006) 919.